

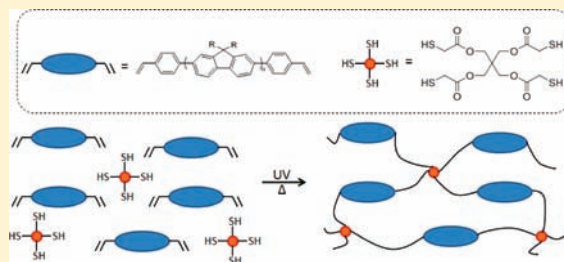
Electroluminescent Networks via Photo “Click” Chemistry

Andrew R. Davis, Janet A. Maegerlein, and Kenneth R. Carter*

Department of Polymer Science and Engineering, University of Massachusetts Amherst, Conte Center for Polymer Research, 120 Governors Drive, Amherst, Massachusetts 01003, United States

S Supporting Information

ABSTRACT: The use of thiol–ene click chemistry is demonstrated for the first time as a suitable method for cross-linking thin films of 4-phenylethenyl end-capped poly(fluorene). Cross-linking was accomplished by a simple, brief UV curing step at modest temperatures. This chemistry provides an advantage over similar schemes employed for cross-linking conjugated polymers since it does not require elevated temperature or produce potentially detrimental side products. Thiol–ene cross-linking was found to preserve the emissive color integrity of the poly(fluorene) films and allowed for facile photopatterning of the active polymer layer. Furthermore, the investigated cross-linking chemistry was shown to be fully compatible with fabrication of polymer light-emitting diodes (PLEDs) whose performance was comparable to noncross-linked devices. Multicolor PLEDs were also demonstrated by taking advantage of the photopatternability of the thiol–ene based system.



INTRODUCTION

In this report, we demonstrate the use of thiol–ene click chemistry to form robust, device-compatible cross-linked films of a conjugated polymer (CP). Poly(dialkyl fluorene)s are a class of material that has been extensively investigated for use in polymer light-emitting diode (PLED) applications due to their deep blue emission, chemical and thermal stability, ease of functional tuning at the 9- position, and high photoluminescent yields.¹ One drawback of poly(fluorene)s is the exhibition of a broad green emission band between 500 and 550 nm which has been attributed to the formation of aggregates and/or the generation of ketone defects.² Cross-linking of CP films has been shown to provide more stable emission due to polymer chains being “locked” into position, significantly reducing their tendency to realign during annealing or device operation.³ Cross-linking also allows for the formation of dual-layer devices where the robust cross-linked layer will not be dissolved during solution processing of a second layer. Additionally, cross-linking enables the incorporation of a wide range of chemical functionality that can be imbedded in the polymer during curing.

Several methods can be found in the literature describing the cross-linking of CP films. The thermally initiated free-radical autopolymerization of styrene is widely known, and there is already a considerable amount of work exploiting this chemistry to cross-link 4-phenylethenyl end-capped CPs such as poly(fluorene)s,⁴ poly(phenylene vinylene)s,⁵ triaryl amines,⁶ and heteroleptic iridium complexes.⁷ While this chemistry is attractive as it requires no additional cross-linking reagents and no side products are anticipated, curing requires an oxygen-free

environment with high temperatures (above 150 °C) and reaction times up to several hours.

To circumvent these concerns, several different UV-initiated cross-linking chemistries have been investigated with poly(fluorene), allowing for curing at lower temperatures and with shorter reaction times. UV-initiated curing gives the added benefit for photopatterning, providing the potential for the fabrication of materials with more complex architectures. One example found in the literature is acrylates, readily polymerized by a radical mechanism which can be initiated photochemically.⁸ Oxetanes, strained four-member cyclic ethers that can undergo cationic ring-opening polymerization, have similarly been used as cross-linkable functional groups, provided a suitable initiator is added.⁹ While UV-initiated cross-linking removes the need for high heat and long reaction times, the curing procedures require some mechanism for initiation. Generally this is achieved by adding a photoacid or photoradical generator (PAG/PRG) to the reaction mixture which acts as an initiator upon UV exposure. It is easy to imagine that this small-molecule additive may result in several deleterious effects including residual initiator and/or undesired side products.

In this work, we aim to investigate a new cross-linking chemistry for CPs that takes advantage of the low curing temperatures and quick processing time provided by UV-curing but proceeds by click chemistry to avoid the problems related to systems utilizing PAG/PRGs. Thiol–ene click chemistry has grown tremendously in popularity over the past few years and has been shown to possess various advantages such as rapid reaction rates, minimal oxygen

Received: September 20, 2011

Published: October 17, 2011

inhibition, and high yields.¹⁰ Because the initiation proceeds by UV-induced homolytic cleavage of the S–H bond, thiol–ene chemistry is advantageous for CP cross-linking as it does not require high temperatures such as those needed for the thermal initiation of 4-phenylethenyl groups and mitigates potential issues with residual PAG/PRG additives. Furthermore, thiol–ene chemistry is well-suited to patterning by photolithography as shown by Hagberg et al.¹¹ To the best of our knowledge, this chemistry has not yet been demonstrated for CP cross-linking. Herein we report on the use of thiol–ene chemistry to photochemically cross-link a thin film of 4-phenylethenyl end-capped poly(dihexyl fluorene) (xDHF). Additionally, cross-linked PLED devices were created to demonstrate the use of this chemistry in active devices.

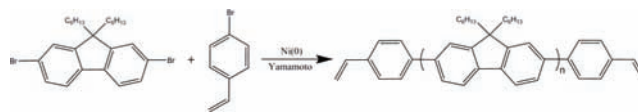
RESULTS AND DISCUSSION

Synthesis. xDHF was synthesized by conventional Yamamoto coupling of 2,7-dibromo-9,9-dihexyl-9H-fluorene with the addition of 4-bromostyrene as an end-capping species with good yield (81%) (Scheme 1). ¹H NMR of synthesized xDHF (Figure S1 in Supporting Information [SI]) showed the desired product with clearly visible vinylic proton resonances ($\delta = 5.3, 5.9, 6.8$ ppm) from the end-groups. Molecular weight and degree of polymerization (DP) of xDHF was calculated by taking the ratio of these vinylic proton signals to the methylene proton of the 9-position hexyl chain α to the fluorene backbone $[-(\text{CH}_2)-(\text{CH}_2)_4-\text{CH}_3]$ and were found to be $M_n = 4500$ kDa and $\text{DP} = 13$. The considerably larger molecular weight of $M_n = 10400$ determined from gel permeation chromatography (GPC) (Figure S2 in SI) can be explained by the rigid nature of poly(fluorene) compared to that of polystyrene standards. The relatively low molecular weight was chosen to allow for a greater cross-linking density (since cross-linking occurs at the chain ends) as well as to limit polydispersity which is known to adversely affect PLED performance.¹² Furthermore, the modest glass transition temperature T_g of xDHF at 85 °C (by differential scanning calorimetry) and its high thermal stability (Figure S3 in SI) are factors that prove advantageous for cross-linking by arguments of increased chain mobility as discussed later.

Cross-Linking of xDHF Films. The overall thiol–ene reaction scheme enabling cross-linking of xDHF is illustrated in Scheme 2. Cross-linking of xDHF films was achieved by spin-coating a solution containing both xDHF and a tetra-functional thiol cross-linker, pentaerythritol tetrakis(3-mercaptopropionate) (PTMPA). An excess of PTMPA (thiol/vinyl = 2:1) was used to ensure that the maximum number of vinyl end groups could find a cross-linker during the thiol–ene click reaction. Upon exposure of the film to UV light, homolytic cleavage of the S–H bond followed by radical reaction with a vinyl end group of xDHF resulted in a cross-linked film. Curing was simple and reproducible via exposure to UV light for as little as 1 min at the polymer's T_g of 85 °C. These conditions are notably milder than thermal cross-linking previously reported for 4-phenylethenyl end-capped poly(fluorene)s.⁴ The extent of cross-linking was monitored qualitatively by a combination of FTIR, film thickness measurements, differential scanning calorimetry (DSC), and film insolubility.

Figure 1 shows the FTIR spectra of the xDHF films before and after cross-linking, where the vinyl C–H peaks at 908 cm^{-1} and 988 cm^{-1} as well as the S–H peak of free thiol at 2577 cm^{-1} are all observed to decrease in intensity following curing. This clearly corresponds to a successful click event where a C–S–C linkage is formed between PTMPA and xDHF vinyl end groups.

Scheme 1. Synthesis of xDHF via Yamamoto Coupling



Scheme 2. (Top) Thiol–Ene Click Reaction between the Vinyl Group of End-Capped Poly(9,9-dihexyl fluorene) (xDHF) and One Thiol of Pentaerythritol Tetrakis(3-mercaptopropionate) (PTMPA); (Bottom) Full Cross-Linking

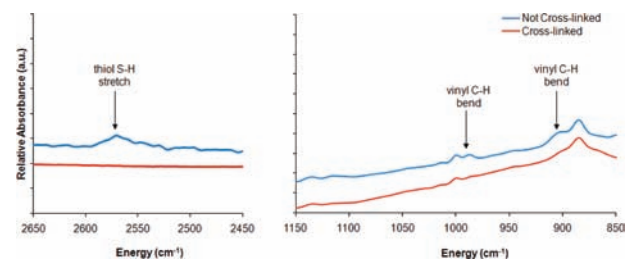
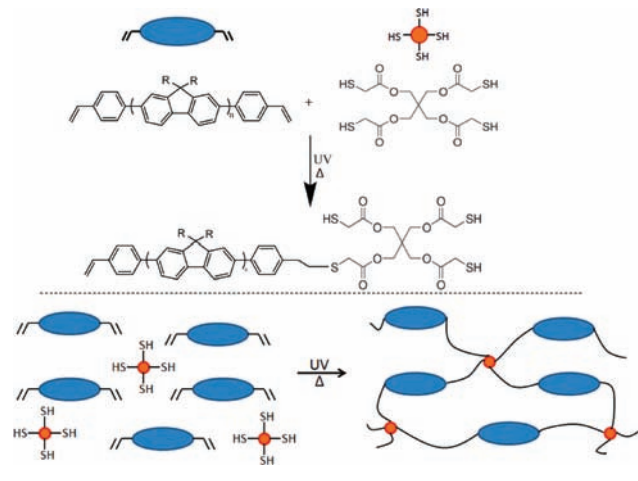


Figure 1. FTIR spectra of xDHF films before and after UV cross-linking. The reduction of the vinyl C–H bending peaks and thiol S–H stretching peak is indicative of successful cross-linking through the vinyl end groups of xDHF.

Following successful cross-linking, films were observed to be insoluble in solvents that were good for the precured resin (e.g., THF, CHCl_3). However, we observed decreased thicknesses both immediately after curing and again when rinsed with solvent. Thus, initial decrease in thickness following curing must be due to both shrinkage during network formation, and the loss of some non-cross-linked material. Film thicknesses after cross-linking and solvent rinsing are shown in Figure 2 as a function of substrate temperature during curing. Reduced film thicknesses observed with decreasing temperature are indicative of material loss due to reduced extent of cross-linking. As the films are heated below T_g (85 °C) during curing, chain mobility is reduced such that the xDHF end-groups are less likely to encounter an active thiol cross-linker during the brief UV exposure. Curing at 75 °C resulted in a cross-linked film that was roughly half as thick as one

cured at 85 °C, and curing at 65 °C showed no measurably cross-linked xDHF film. Curing at temperatures above 85 °C did not significantly increase final film thickness, suggesting that the full extent of cross-linking can be achieved at T_g of the polymer.

Cross-linking of xDHF was additionally investigated using photo and modulated DSC. Photo DSC results (Figure 3) show how rapid the UV-initiated reaction occurs, with completion in only 6 s upon exposure to 365 nm light (6 mW/cm^2) with the sample held at an isotherm of 85 °C. This is consistent with the very rapid rates of thiol–ene polymerization previously reported.¹⁰ Curing with 254 nm light, which more efficiently cleaves the S–H thiol bond,¹⁰ would likely lead to even more effective cross-linking. The inset of Figure 3 shows high-temperature modulated DSC results for a previously UV-cross-linked sample (solid line) and

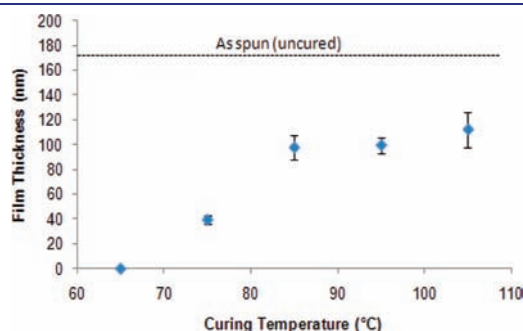


Figure 2. Thicknesses of xDHF films as a function of curing temperature.

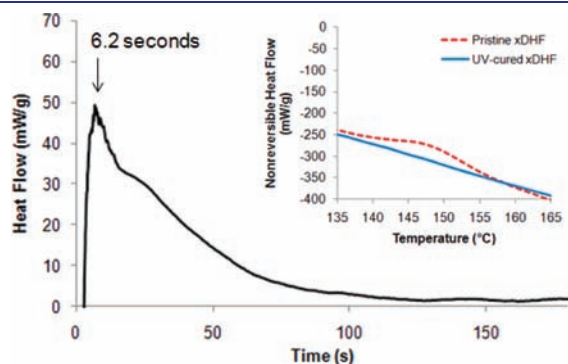


Figure 3. Photo DSC response of xDHF with cross-linking thiol upon exposure to 365 nm UV light. (Inset) High temperature-modulated DSC response of pristine xDHF (dashed line) and UV-cured xDHF (solid line).

pristine xDHF (dashed line). The exotherm near 150 °C for the pristine xDHF confirms cross-linking achieved by the autoinitiation of xDHF end-capping groups. The lack of a similar exotherm for the UV-cured xDHF provides further evidence that all accessible cross-linking sites have reacted during UV curing. As evidenced by FT-IR data, it appears that some residual vinyl functionality does exist in the cured xDHF films. In this case we attribute the lack of high-temperature isotherm to isolated unreacted styrene end-groups that, once incorporated into the cross-linked network, lack the necessary mobility to reach similarly unreacted end groups.

The UV–vis absorption and photoluminescence (PL) of the xDHF polymer are shown in Figure 4. Both UV–vis absorption and PL were found to red-shift from solution state to solid film, as would be expected upon the formation of lower-energy states in the aggregated solid state. Furthermore, UV cross-linking of the xDHF film was not found to adversely affect emissive behavior, with cured and uncured films showing an identical peak emission at 424 nm. In fact, UV curing of the spun films seems to somewhat suppress lower-energy emissions, likely due to xDHF chains being locked into a rigid matrix, preventing rearrangement to lower-energy aggregate states. In order to confirm the advantageous effects of thiol–ene cross-linking on emissive color stability, we examined various xDHF films under high-temperature annealing conditions. When annealed in nitrogen for 1 h at 150 °C, as-spun films of pristine xDHF and xDHF mixed with PTMPA both show increasing green emission near 520 nm. Thus, the presence of the unreacted small-molecule cross-linker is not alone sufficient to inhibit aggregation. Thermally cross-linked films (with no added thiol cross-linker) show a large peak at 520 nm both before and after annealing (Figure 5). Since thermal cross-linking necessitated heating of a pristine xDHF above 150 °C, introduction of lower-energy aggregates during the curing procedure is inevitable. Thus, it is not surprising that a large amount of green emission is observed in the preannealed film. By comparison, UV-initiated thiol–ene cross-linked films show no increased green emission even after high-temperature annealing. The low curing temperature coupled with formation of a rigid cross-linked matrix is thus effective at preventing aggregation, consistent with other studies of poly(fluorene) networks.⁴

Light-Emitting Diodes and Patterned Structures. In addition to the formation of patterned CP films using xDHF, we also demonstrated that the thiol–ene cross-linking chemistry is fully compatible with organic electronic devices. Figure 6 and Figure 7 show the current density–voltage–luminance (J – V – L) and electroluminescence (EL) behavior of PLEDs fabricated using xDHF as an active layer. Devices were compared using xDHF either directly as spun, cross-linked via UV exposure as described above, or cross-linked thermally at elevated temperatures without

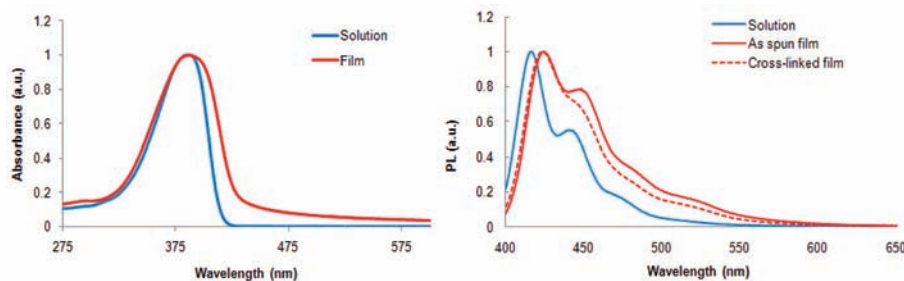


Figure 4. UV–vis absorption (left) and photoluminescence (PL) of xDHF in both the solution and solid state. PL is also shown for the thiol–ene cross-linked xDHF film.

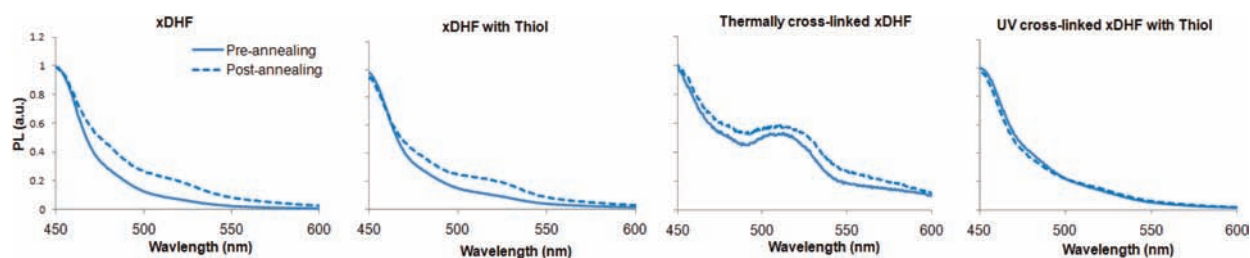


Figure 5. Photoluminescence of various xDHF films before (solid lines) and after (dashed lines) annealing at 150 °C under N_2 .

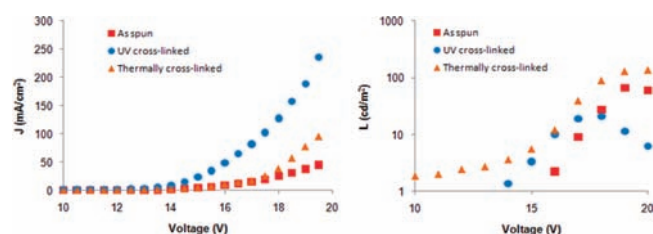


Figure 6. Current density (J) and luminance (L) response for PLEDs with xDHF as the active layer as a function of operating voltage. Devices were fabricated with either as spun xDHF, thermally cross-linked xDHF, or UV-initiated thiol–ene cross-linked xDHF.

added PTMPA (under N_2 by autoinitiation of styrenic end groups).

J – V – L behavior of the PLEDs shows that cross-linking does not significantly affect turn-on voltages of the devices, with all devices turning on near 15 V, a somewhat high operating voltage, but one that is consistent among tested devices. The UV cross-linked xDHF PLEDs were found to display comparable brightness to those of as-spun or thermally cross-linked devices, especially at lower operating voltages. Device performance would no doubt be improved with further optimization of film and cathode thicknesses. Relatedly, it is possible that higher-molecular weight xDHF would also improve device performance. However, this would potentially come at the cost of poorer curing properties due to dilution of the reactive vinyl end groups.

The EL profiles retain the same general line shape following curing, suggesting that thiol–ene cross-linking does not degrade emissive color. One difference between devices is particularly noteworthy: devices fabricated via thiol–ene cross-linking do not show the increased green emission near 480 nm that is evident with thermal cross-linking, similar to the above photoluminescent behavior. This undesired green emission has long been reported in poly(fluorene) emission,^{2a–c} and it is not surprising that the high temperature of thermal curing at 200 °C increases its intensity due to the formation of low-energy aggregates and/or fluorenone defects. The more moderate temperatures required for UV-initiated thiol–ene chemistry allow for cross-linking of the active film without introduction of this undesired green emission.

Finally, the opportunity for using UV-curable xDHF as a photopatternable active layer was demonstrated in both a thin film of xDHF on a silicon wafer and in a multicolor PLED (Figure 8) using an arbitrary photomask to create patterned CP films. Figure 8a shows the resulting fluorescent pattern after cross-linking on Si, where the bright-blue regions are areas of cross-linked polymer fluorescing under UV light. Dark regions were masked (and thus not cross-linked) during curing, and the uncured xDHF was easily rinsed away with THF, leaving no

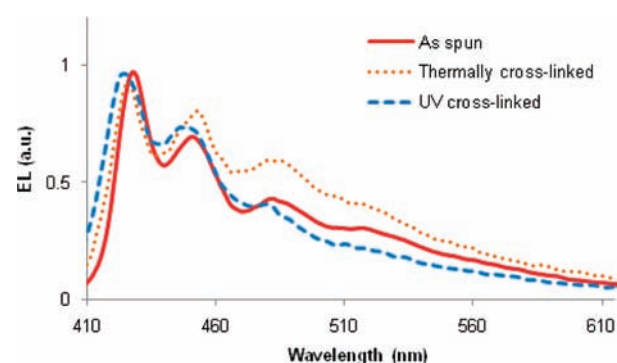


Figure 7. Electroluminescence (EL) profiles of various PLEDs using xDHF as the emissive layer. Devices were fabricated with either as spun xDHF, thermally cross-linked xDHF, or UV-initiated thiol–ene cross-linked xDHF. PLED structure was ITO/PEDOT:PSS/xDHF/Ca/Al in all cases.

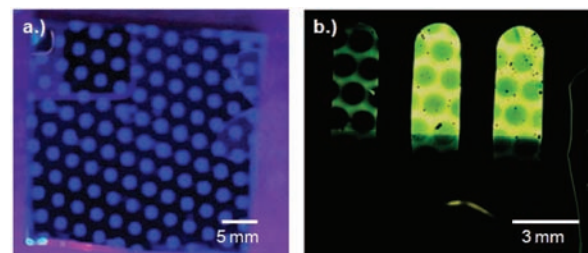


Figure 8. Photopatterned xDHF film on Si (a) and PLED (b) with the device structure ITO/PEDOT:PSS/xDHF(circles)/PFBT/Ca/Al. For PLEDs, emission from only the PFBT regions was observed at lower voltages (left device), while emission across the entire device was seen at larger operating voltages (right two devices).

emissive polymer. The ability to use a photomask to create any desired CP pattern is a significant advantage of the thiol–ene chemistry over thermally activated cross-linking systems.

Using the same photomask, circular patterns of xDHF were fabricated on an ITO substrate, and a bilayer device was created via the subsequent spin-coated deposition of poly(fluorene-co-benzothiadiazole) (PFBT) from chloroform. The preservation of the xDHF patterns after an additional processing step in chloroform (a good solvent for uncured xDHF) further proves their robustness. It is interesting to note that, at low operating voltages (<15 V), electroluminescence was observed only in the PFBT-coated regions (left device, Figure 8b). With increased operational voltage (>15 V), the entire device was seen to emit (right devices, Figure 8b). Since single-layer xDHF devices were observed to turn on at approximately 15 V, we attribute this behavior primarily to

differences in energy levels between xDHF and PFBT. As measured by cyclic voltammetry, HOMO/LUMO levels of xDHF were found to be 5.39 and 2.42 eV respectively (Figure S4 in SI) compared to PFBT HOMO/LUMO energies of 5.9 and 3.2 eV.¹³ Given the 2.9 eV work function of the calcium cathode, we expect a lower-energy barrier for charge carrier injection into the PFBT layer than the xDHF layer. This could explain the partial emission we observed below 15 V.

CONCLUSIONS

We have demonstrated the use of UV-initiated thiol–ene cross-linking of 4-phenylethenyl end-capped poly(dihexyl fluorene). To our knowledge, this is the first reported use of thiol–ene click chemistry to form cross-linked emissive CP networks. Characteristic of click chemistry, network formation is simple and rapid, with curing accomplished in a matter of seconds at modest temperatures that are not detrimental to emissive color. Furthermore, cross-linking was shown to enhance color stability at high temperature. Additionally, cross-linked CP films are fully compatible with electroluminescent devices, and their performance is comparable to that of uncured devices. Photocuring of these films provides the advantage of patternability, and we have shown that an arbitrary pattern can be generated in the xDHF layer by use of a photomask (results unachievable with thermally cross-linkable chemistries). This allows for a new chemical avenue toward pixilated multicolor displays. We are currently investigating this new chemistry with lower band gap polymers to create patterned transistor and photovoltaic devices. This new moderate temperature photocuring reaction also makes these materials extremely attractive for roll-to-roll processes on flexible substrates.

EXPERIMENTAL SECTION

Materials. 4-Bromostyrene, 2,7-dibromo-9,9-dihexyl-9H-fluorene (DBDHF), 2,2'-bipyridyl (BPY), 1,5-cyclooctadiene (COD), tetrahydrofuran (THF), pentaerythritol tetrakis-(3-mercaptopropionate), and poly(3,4-ethylenedioxythiophene)/poly(styrenesulfonate) (PEDOT/PSS) were purchased from Sigma-Aldrich Company. DBDHF was recrystallized from ethanol prior to use. The active Ni(0) coupling reagent, bis(1,5-cyclooctadiene)nickel(0) [Ni(COD)₂], was purchased from Strem Chemicals and handled under inert atmosphere. Anhydrous toluene and dimethylformamide (DMF), stored under nitrogen over molecular sieves, were purchased from Sigma Aldrich Company. All reagents were used as received unless otherwise noted. Silicon substrates were purchased from University Wafers. Indium tin oxide (ITO)-coated glass was purchased from Thin Film Devices, Inc. (sheet resistance 20 Ω/□). All reactions were run under dry N₂ unless otherwise noted.

Instrumentation. All nuclear magnetic resonance (NMR) spectra were acquired on a Bruker AF 300 (300 MHz) spectrometer and internally referenced via residual solvent signal [CHCl₃: ¹H 7.24 ppm; ¹³C 77.00 ppm]. All chemical-shift values are given in ppm. Gel permeation chromatography (GPC) was performed in THF at room temperature with 1.0 mL/min elution rate. A Waters R403 differential refractometer and three PLgel columns (105, 104, and 103 Å) calibrated with narrow molecular weight polystyrene standards were used. Differential scanning calorimetry (DSC) was performed on a Thermal Analysis (TA) Q-2000 in T-zero aluminum pans using modulated DSC at 3 °C/min. Thermal gravimetric analysis was performed using a Perkin-Elmer TGS-2, under nitrogen atmosphere with a heating rate of 10 °C/min.

Film thicknesses were measured by profilometry using a Dektak 150 profilometer. UV–vis spectra were recorded in 1-cm path length quartz cuvettes. Fluorescence measurements were taken on a Perkin-Elmer

LS-50B. Infrared spectroscopy of polymer films was performed on a Nicolet 6700 FT-IR spectrometer with a Harrick grazing angle ATR accessory (GATR).

Microwave Reactor. Microwave heating was performed in a Smith-Creator single-mode microwave cavity producing continuous radiation at a frequency of 2.45 GHz (Personal Chemistry, Inc. Reactions were conducted under nitrogen in 35-mL, heavy-walled pyrex glass reaction vials sealed with silicone caps fitted with a silicone septum. Reaction mixtures were stirred internally with a magnetic stir bar during the irradiation.

Polymerization of Styrene End-Capped 2,7-Dibromo-9,9-dihexyl-9H-fluorene (xDHF). Cross-linkable, end-capped homopolymer (xDHF) was synthesized by the nickel(0)-mediated polymerization of 2,7-dibromo-9,9-dihexyl-9H-fluorene (DBDHF) and 4-bromostyrene via microwave heating. DBDHF (300 mg, 0.609 mmol, 1 equiv) and 2,2'-dipyridyl (257 mg, 1.645 mmol, 2.87 equiv) were added to a 35-mL microwave vial. In a glovebox, Ni(COD)₂ (409 mg, 1.487 mmol, 2.44 equiv) and a stirbar were added to the vial which was then sealed. 4-Bromostyrene (12.2 μL, 0.06 mmol, 0.125 equiv), COD (191 μL, 1.554 mmol, 2.55 equiv), and 15 mL of dry toluene/DMF (3:1 v/v) were injected, and the vial was degassed and backfilled with nitrogen three times. The reaction was heated in a microwave at 100 °C for 30 min after 30 s of pre-stirring. After reaction, the polymer solution was filtered through a syringe filter (0.45 μm) and precipitated by adding it dropwise into 300 mL of methanol and conc. HCl (98:2 v/v). The crude polymer was dissolved in minimal THF and reprecipitated into methanol. The recovered light-yellow precipitate was dried overnight under vacuum (170 mg, 81% yield). ¹H NMR (300 MHz, CDCl₃) δ 7.86–7.68 (40H, aromatic); 6.84, 5.86, 5.32 (dd 1H, d 1H, d1H, vinyl end-caps); 2.11, 1.14, 0.80 (24H, 72H, 60H, alkyl chain). DP via ¹H NMR 13; M_n via GPC 10400; PDI 2.31.

Film Coating and Cross-Linking. Silicon wafers were solvent rinsed sequentially with hexanes, acetone, THF, water, and 2-propanol and then dried under a stream of nitrogen. Subsequently, the substrate was soaked in a piranha bath (5:1 concentrated sulfuric acid:30% hydrogen peroxide) at 100 °C for 30 min, rinsed thoroughly with DI water, and dried under nitrogen. xDHF solutions were made by dissolving 15 mg of polymer in 500 μL of CHCl₃ and then adding 500 μL of toluene. In the case of thermally cross-linkable films, no further reagents were added. In the case of UV-curable films, the tetrafunctional cross-linker, pentaerythritol tetrakis-(3-mercaptopropionate), was added in a stoichiometric amount (1:2 vinyl/thiol) as a solution in toluene. Solutions were spin-coated onto the cleaned wafers at 2000 rpm for 60 s. Thermal cross-linking was carried out on a hot plate at 200 °C for 45 min under a nitrogen atmosphere to form an insoluble layer. UV cross-linking was accomplished at 85 °C for 5 min in a nitrogen atmosphere under 365-nm light unless noted otherwise, forming an insoluble layer. All films were rinsed with THF and dried under a stream of nitrogen to ensure all uncross-linked material was removed from the surface.

Device Fabrication. Polymer light-emitting diodes (PLEDs) were fabricated using xDHF as the active emitting layer. ITO-coated glass was first solvent cleaned and subsequently treated with O₂ plasma for 3 min. Poly(ethylene-dioxythiophene)/poly(styrenesulfonate) (PEDOT/PSS) (1.3 wt % in H₂O, Aldrich) was then spin-coated at 4000 rpm and dried under N₂ at 150 °C for 30 min. Solutions of xDHF were then spun from a mixed solution of chloroform and toluene containing pentaerythritol tetrakis-(3-mercaptopropionate) tetra-functional cross-linker, such that the ratio of –SH groups to xDHF vinyl groups was 2:1 to ensure complete cross-linking. UV cross-linked devices were then heated to 85 °C under N₂ and exposed to a 365 nm UV light source for 5 min. Thermally cross-linked devices were cured at 200 °C under N₂ for 1 h. All cross-linked devices were then rinsed with THF and dried under vacuum overnight. As spun devices were simply placed under vacuum overnight directly following spin-coating. In order to ensure all devices had comparably thick active layers, spin-coating speeds for the active

layer solution was varied for each treatment to account for losses in thickness during curing. Devices were completed by the thermal evaporation of 15 nm Ca cathodes capped with 100 nm Al at pressure $<10^{-5}$ Torr with active areas of 0.15 cm^2 . Devices were tested in air using a Keithley 2602 Sourcemeter and a calibrated Ocean Optics USB4000 UV-vis spectrometer.

Patterned PLEDs were fabricated using a photomask during UV curing of the xDHF layer to selectively cross-link xDHF circles. Substrates were rinsed in THF to remove uncured xDHF, and a solution of poly(flourene-co-benzothiadiazole) in chloroform was subsequently spun on the substrates. Drying, cathode deposition, and testing were completed as above.

■ ASSOCIATED CONTENT

S Supporting Information. Additional polymer characterization. This material is available free of charge via the Internet at <http://pubs.acs.org>.

■ AUTHOR INFORMATION

Corresponding Author

krcarter@polysci.umass.edu

■ ACKNOWLEDGMENT

We thank the National Science Foundation (DMR-0906695) for support.

■ REFERENCES

- (1) (a) Fukuda, M.; Sawada, K.; Yoshino, K. *Jpn. J. Appl. Phys.* **1989**, *28*, L1433–L1435. (b) Pei, Q.; Yang, Y. *J. Am. Chem. Soc.* **1996**, *118*, 7416–7417.
- (2) (a) Romaner, L.; Pogantsch, A.; Scandiucci de Freitas, P.; Scherf, U.; Gaal, M.; Zojer, E.; List, E. J. W. *Adv. Funct. Mat.* **2003**, *13*, 597–601. (b) Weinfurter, K.-H.; Fujikawa, H.; Tokito, S.; Taga, Y. *Appl. Phys. Lett.* **2000**, *76*, 2502–2504. (c) Bliznyuk, V. N.; Carter, S. A.; Scott, J. C.; Klärner, G.; Miller, R. D.; Miller, D. C. *Macromolecules* **1999**, *32*, 361–369. (d) Gong, X.; Parameswar, K. I.; Moses, D.; Guillermo, C. B.; Heeger, A. J.; Xiao, S. S. *Adv. Funct. Mat.* **2003**, *13*, 325–330.
- (3) Zhao, W.; Cao, T.; White, J. M. *Adv. Funct. Mat.* **2004**, *14*, 783–790.
- (4) (a) Chen, J. P.; Klaerner, G.; Lee, J.; Markiewicz, D.; Lee, V. Y.; Miller, R. D.; Scott, J. C. *Synth. Met.* **1999**, *107*, 129–135. (b) Klärner, G.; Lee, J.-I.; Lee, V. Y.; Chan, E.; Chen, J.-P.; Nelson, A.; Markiewicz, D.; Siemens, R.; Scott, J. C.; Miller, R. D. *Chem. Mater.* **1999**, *11*, 1800–1805. (c) Bozano, L. D.; Carter, K. R.; Lee, V. Y.; Miller, R. D.; Dipietro, R.; Scott, J. C. *J. Appl. Phys.* **2003**, *94*, 3061–3068.
- (5) Sun, H.; Liu, Z. E.; Hu, Y.; Wang, L.; Ma, D.; Jing, X.; Wang, F. *J. Polym. Sci., Part A: Polym. Chem.* **2004**, *42*, 2124–2129.
- (6) (a) Paul, G. K.; Mwaura, J.; Argun, A. A.; Taraneekar, P.; Reynolds, J. R. *Macromolecules* **2006**, *39*, 7789–7792. (b) Niu, Y.-h.; Liu, M. S.; Ka, J.-w.; Jen, A. K. *Appl. Phys. Lett.* **2006**, *88*, 093505–093507.
- (7) Ma, B. B.; Kim, B. J.; Poulsen, D. A.; Pastine, S. J.; Fre, J. M. *J. Adv. Funct. Mat.* **2009**, *19*, 1024–1031.
- (8) (a) Scheler, E.; Bauer, I.; Strohmriegl, P. *Macromol. Symp.* **2007**, *254*, 203–209. (b) Scheler, E.; Strohmriegl, P. *J. Mater. Chem.* **2009**, *19*, 3207–3212.
- (9) Bayerl, M. S.; Braig, T.; Nuyken, O.; Mu, D. C.; Groß, M.; Meerholz, K. *Macromol. Rapid Commun.* **1999**, *20*, 224–228.
- (10) (a) Posner, T. *Chem. Ber.* **1905**, *38*, 646–657. (b) Kaneko, T. *J. Chem. Soc. Jpn.* **1938**, *59*, 1139–1141. (c) Cramer, N. B.; Scott, J. P.; Bowman, C. N. *Macromolecules* **2002**, *35*, 5361–5365. (d) Iha, R. K.; Wooley, K. L.; Nyström, A. M.; Burke, D. J.; Kade, M. J.; Hawker, C. J. *Chem. Rev.* **2009**, *109*, 5620–5686. (e) Lowe, A. B. *Polym. Chem.* **2010**, *1*, 17–36. (f) Hoyle, C. E.; Bowman, C. N. *Angew. Chem., Int. Ed.* **2010**,

49, 1540–1573. (g) Hoyle, C. E.; Lowe, A. B.; Bowman, C. N. *Chem. Soc. Rev.* **2010**, *39*, 1355–1387.

(11) Hagberg, E. C.; Malkoch, M.; Ling, Y.; Hawker, C. J.; Carter, K. R. *Nano Lett.* **2007**, *7*, 233–237.

(12) Skotheim, T. A.; Reynolds, J. R. *Handbook of Conducting Polymers*; CRC Press: Boca Raton, FL, 2007.

(13) Campbell, A. J.; Bradley, D. D. C.; Antoniadis, H. *Appl. Phys. Lett.* **2001**, *79*, 2133–2135.

■ NOTE ADDED AFTER ASAP PUBLICATION

This article was published ASAP on November 22, 2011. The abstract graphic and Scheme 2 have been updated. The corrected version was posted on November 29, 2011.